Article

GPU Based Modelling and Analysis for Parallel Fractional Order Derivative Model of the Spiral-Plate Heat Exchanger

Guanqiang Dong [ID] **and Mingcong Deng** *[ID]

The Graduate School of Engineering, Tokyo University of Agriculture and Technology, Tokyo 184-8588, Japan; guanqiangdong@gmail.com
* Correspondence: deng@cc.tuat.ac.jp

Abstract: Heat exchangers are commonly used in various industries. A spiral-plate heat exchanger with two fluids is a compact plant that only requires a small space and is excellent in high heat transfer efficiency. However, the spiral-plate heat exchanger is a nonlinear plant with uncertainties, considering the difference between the heat fluid, the heated fluid, and other complex factors. The fractional order derivation model is more accurate than the traditional integer order model. In this paper, a parallel fractional order derivation model is proposed by considering the merit of the graphics processing unit (GPU). Then, the parallel fractional order derivation model for the spiral-plate heat exchanger is constructed. Simulations show the relationships between the output temperature of heated fluid and the orders of fractional order derivatives with two directional fluids impacted by complex factors, namely, the volume flow rate in hot fluid, and the volume flow rate in cold fluid, respectively.

Keywords: fractional order derivative model; GPU; a spiral-plate heat exchanger; parallel model; heat transfer; nonlinear system

1. Introduction

A heat exchanger is most often used in industries such as space heating, refrigeration, air conditioning, power stations, chemical plants, petrochemical plants, petroleum refineries, natural-gas processing, and sewage treatment. It uses the principle of heat transfer between two or more fluids to transfer the heat energy of the high temperature heat fluid to the low temperature heat fluid in order to heating the low temperature fluid or cooling the high temperature heat fluid, which has the idea of energy saving [1]. A spiral-plate heat exchanger is a compact plant that only requires a small space for installation compared to traditional heat exchanger solutions and has excellent in high heat transfer efficiency (See [2–4]). However, the spiral-plate heat exchanger is a nonlinear plant with uncertainties, considering the difference between the heat medium, the heated medium and the other factors. In some applications, the output temperature heated or cooled for the heat exchanger must be controlled accurately. Because the heat transfer coefficient of the heat exchanger is impacted by various factors such as fluid flow, condition pressure, the uncertainties, the error of the mathematical model, and a long-time delay, etc., so it is difficult to be accurately modelled and controlled. In the past few years, the research of heat exchangers has mainly focused on the design of heat exchangers [5–7]. In some papers (Such as [8,9]), an effective internal fluid mathematical model is established by using the heat balance law between the two fluids. Only the effect of the flow velocity on the heat transfer coefficient, but not the effect of the two fluid flows velocity on the heat transfer time is considered.

Fractional order calculus and derivative is a old topic of a more than 300 years since a letter written by Leibniz to L'Hopital in 1695 [10]. Fractional order calculus is an extension from traditional integer calculus. The research of the theory and applications of fractional order calculus and derivatives (such as in solution of fractional order calculus and derivative [11,12] and stability [13–15]) expanded greatly over the 20th and 21st centuries.

In recent years, fractional order calculus and derivatives have been used in various fields such as engineering, physics, chemistry, and hydrology etc. The references in [10,16], give some knowledges about fractional order calculus and derivative. The fractional order PID controller was introduced by Podlubny in 1994 [10]. Fractional order controllers were being used extensively by many researchers to achieve the better robust performance in both the linear and the nonlinear systems. In [17], nonlinear thermoelastic fractional-order model of nonlocal plates is studied. The reference [18] proposed a fractional nonlocal elasticity model. They show elasticity model described by fractional order derivative is more accurate than the traditional system described by integer order in theory and application [19]. In control systems, modelling, stability, controllability, observability is very important for performance. In fractional order system, these need to be considered in [20–22], too. Nowadays, fractional order calculus and derivative are still the absence of solution method and rapid computing algorithm [23].

GPU (That is graphics processing unit), which provides more computing units and high data bandwidth in a limited area [24]. It is originally developed for graphics applications, now, it has been increasingly applied to do parallel computing in scientific and engineering. GPU has higher execution efficiency for parallel data, and the more data parallelism, the higher the execution efficiency. CUDA is a software and hardware system that can make GPU work as a device for data parallel computing [25].

References [20,26–28] show elasticity model described by fractional order derivative is more accurate than the traditional system described by integer order in theory and application. Fractional order derivative equation is more suitable to describe thermoelastic model than integer order equation. Heat transfer for the heat exchanger is thermoelastic model. Therefore, it is motivated by the above references. Traditionally, a spiral-plate heat exchanger mathematical model is constructed by integer order derivative equation. A spiral-plate heat exchanger mathematical model constructed by fractional order derivative equation is more accurate than conventional method. So, a parallel fractional order derivative model is proposed by considering the merits of GPU and fractional order derivative. Further, parallel fractional order derivation model for the spiral heat exchanger is constructed. The parallel fractional order derivation model for the spiral-plate heat exchanger executes faster than traditional model and can quickly reply to disturbance. In the future, we will study operator-based robust nolinear control system for the spiral heat exchanger by using the proposed parallel model [29–31].

The rest of this paper is constructed as follows. In Section 2, Preliminaries and Problem Statement, a parallel fractional order derivative model is proposed, and the problem statement is presented. A mathematic fractional order derivative model for the spiral-plate heat exchanger is derived in Section 3, Mathematics Analysis. The proposed parallel model for the spiral-plate heat exchanger with both the counter-flow type and the parallel-flow type and implementation on GPU are given in Section 4. Then, Section 5 compares the relationships between the output temperature of the heated flow fluid and the orders of the fractional order derivative with the two directional fluids, the volume flow rate of cold fluid, and the volume flow rate of hot fluid, respectively. Finally, in Section 6, a conclusion is given.

2. Preliminaries and Problem Statement

2.1. Parallel Fractional Order Derivative Model

In reference [32], parallel fractional order derivative model is not complete only modelling of a spiral heat exchanger with counter-type by using fractional order equation and without theory support. It is richened to derive this paper.

According to the definition of the fractional order derivative (see Appendix A), the fractional order derivative Equation (1) are given as follows.

$$
\begin{cases}
D_t^q f(\Delta h) = -(\Delta h)^{-q} \frac{\Gamma(q+1)}{\Gamma(2)\Gamma(q)} f(0) + (\Delta h)^{-q} f(\Delta h) \\
D_t^q f(2(\Delta h)) = (\Delta h)^{-q} \frac{\Gamma(q+1)}{\Gamma(3)\Gamma(q-1)} f(0) - (\Delta h)^{-q} \frac{\Gamma(q+1)}{\Gamma(2)\Gamma(q)} f(\Delta h) + (\Delta h)^{-q} f(2(\Delta h)) \\
D_t^q f(3(\Delta h)) = -(\Delta h)^{-q} \frac{-\Gamma(q+1)}{\Gamma(4)\Gamma(q-2)} f(0) + (\Delta h)^{-q} \frac{\Gamma(q+1)}{\Gamma(3)\Gamma(q-1)} f(\Delta h) \\
\qquad\qquad\quad -(\Delta h)^{-q} \frac{\Gamma(q+1)}{\Gamma(2)\Gamma(q)} f(2(\Delta h)) + (\Delta h)^{-q} f(3(\Delta h)) \\
\vdots \\
D_t^q f(N(\Delta h)) = (\Delta h)^{-q} \sum_{j=1}^{N} (-1)^j \frac{\Gamma(q+1)}{\Gamma(j+1)\Gamma(q-j+1)} f(t - j(\Delta h)) + (\Delta h)^{-q} f(N(\Delta h))
\end{cases}
\tag{1}
$$

From (1), a parallel fractional order derivative model is described by the matrix, as follow.

$$
F_k = (\Delta h)^q D_{frac} + B F_{k-1}
\tag{2}
$$

where F_k, F_{k-1}, $D_{frac} \in R^N$, and $B \in R^{N \times N}$

$$
F_k = \begin{pmatrix} f(\Delta h) \\ f(2(\Delta h)) \\ \vdots \\ f(N(\Delta h)) \end{pmatrix}
\tag{3}
$$

$$
D_{frac} = \begin{pmatrix} D_t^q f(\Delta h) \\ D_t^q f(2(\Delta h)) \\ \vdots \\ D_t^q f(N(\Delta h)) \end{pmatrix}
\tag{4}
$$

$$
B = \begin{pmatrix}
\frac{-\Gamma(q+1)}{\Gamma(2)\Gamma(q)} & 0 & \cdots & 0 \\
\frac{\Gamma(q+1)}{\Gamma(3)\Gamma(q-1)} & \frac{-\Gamma(q+1)}{\Gamma(2)\Gamma(q)} & \cdots & 0 \\
\vdots & \vdots & \vdots & \vdots \\
\frac{(-1)^N \Gamma(q+1)}{\Gamma(N+1)\Gamma(q-N+1)} & \frac{(-1)^{(N-1)}\Gamma(q+1)}{\Gamma(N)\Gamma((q-N+1)} & \cdots & \frac{-\Gamma(q+1)}{\Gamma(2)\Gamma(q)}
\end{pmatrix}
\tag{5}
$$

$$
F_{k-1} = \begin{pmatrix} f(0) \\ f(\Delta h) \\ \vdots \\ f((N-1)(\Delta h)) \end{pmatrix}
\tag{6}
$$

2.2. Problem Statement

Traditionally, a spiral-plate heat exchanger mathematical model is constructed described by the integer order derivative equation. The spiral-plate heat exchanger mathematical model described by the fractional order derivative is more accurate than the traditional method. So, a fractional order derivation model is considered to describe a spiral-plate heat exchanger plant. Further, parallel fractional order derivative model is proposed by considering the merit of GPU. The proposed parallel model executes faster than traditional model and can quickly reply to disturbance. Further, we get the parallel fractional order derivative model for the spiral heat exchanger by mathematics analysis.

3. Mathematics Analysis

3.1. A Spiral-Plate Heat Exchanger Plant

A spiral-plate heat exchanger is shown in Figure 1. The spiral-plate heat exchanger is used for its many merits, such as high-efficient heat transfer, small-size in comparison to the other heat exchangers, and self-cleaning due to the special spiral structure.

Figure 1. A spiral-plate heat exchanger plant.

The spiral-plate heat exchanger is an excellent process equipment, but it is difficult to obtain an accurate model due to a complex inner structure. The conventional method, such as logarithmic mean temperature difference method, could not obtain good control results. The other approach was conducted, but the obtained model was too complex. It is difficult to design a model based controller. Therefore, we consider a novel spiral-plate heat exchanger's fractional order derivative model. Figure 2 gives the cross-section inner structure of the spiral-plate heat exchanger. Where δ_h , δ_c δ_s is the width of hot fluid, the width of cold fluid and the width of solid wall, respectively. In this study, the cross-section inner structure as shown in Figure 2 is divided into a micro volume in cold fluid. The fractional order derivative model is constructed by considering the heat balance of the hot fluid and cold fluid, respectively.

$$r = b + a \cdot \theta, \theta \in [0, 11\pi] \tag{7}$$

Geometric parameters of the spiral-plate heat exchanger are denoted in Table 1.

Table 1. Parameters of the spiral heat exchanger.

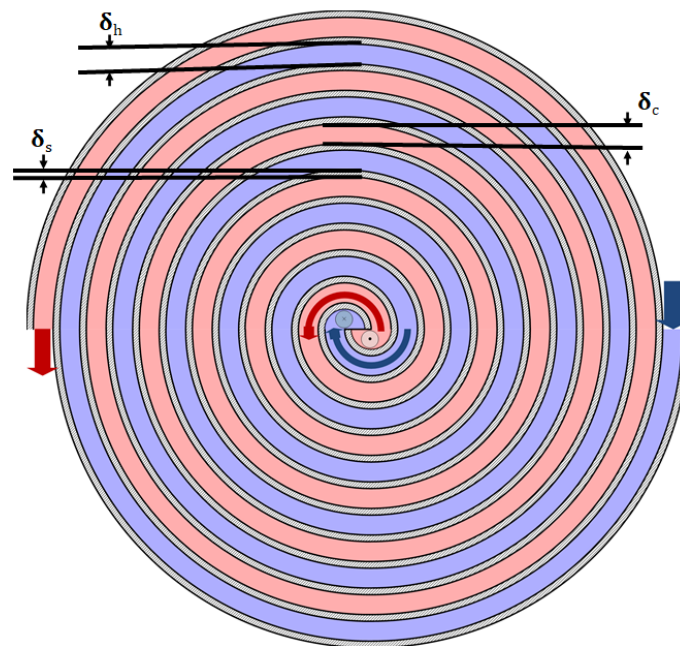| Meaning	Symbol	Value
Geometric parameter of a spiral function	a	$0.005/\pi$ m/rad
Initial radius of hot fluid side	b	0.08 m
The width of hot flow channel	δ_h	0.005 m
The width of cold flow channel	δ_c	0.005 m
The width of solid wall	δ_s	0.0018 m
The height of the spiral-plate heat exchanger	Z	0.011 m

Figure 2. The cross-section inner structure of the spiral heat exchanger.

The heat exchanger is typically classified into the parallel-flow type and the count-flow type by arrangement [33]. The parallel-flow type is that both the input and the output of the two directional fluids (one is a hot fluid, the other is cold fluid) are in the same directions. If both the hot fluid and the cold fluid are in the opposite directions, then it is the counter-flow type heat exchanger. First, fractional order derivative model for the spiral-plate heat exchanger with the counter-flow type is considered.

3.2. Fractional Order Derivative Model for the Spiral-Plate Counter-Flow Heat Exchanger

In this section, the spiral-plate heat exchanger with the counter-flow type is analysed here. First, we consider the temperature variable in cold fluid, that is divided into a micro volume as shown in Figure 3. Here, v_h is the flow rate in hot fluid. v_c is the flow rate in cold fluid. The directions of v_h, and v_c are opposite. ΔV is a micro volume in cold fluid. Δm_1 is the heat flux transferring from the inside $T_h(x)$. Δm_2 is the heat flux transferring from the outside $T_h(x + C)$, C is the length to the angle of 2π.
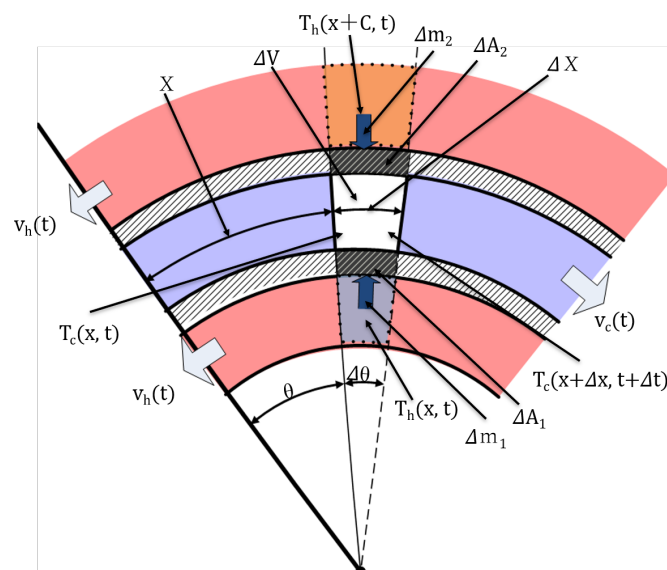

Figure 3. The principle of heat transfer for the spiral heat exchanger.

As seen in Figure 3, it denotes the heat transferring between the two fluids for the spiral-plate counter-flow heat exchanger.

Therefore, according to the heat energy balance law and heat transfer theory [34], the equations are derived as follows.

$$c_c \rho_c (\Delta V) \frac{\Delta T_c(x,t)}{\Delta t} = \Delta m_1 + \Delta m_2 \tag{8}$$

$$\frac{\Delta T_c(x,t)}{\Delta t} = T_c(x + \Delta x, t + \Delta t) - T_c(x,t) \tag{9}$$

where c_c, ρ_c, ΔV, k is the specific heat capacity of cold fluid, the density of cold fluid, a micro volume, the heat transfer coefficient of the spiral-plate heat exchanger, respectively. According to the Newton's law of cooling.

$$k = \frac{1}{h_h} + \frac{\delta_s}{\lambda} + \frac{1}{h_c} \tag{10}$$

where h_h, h_c, δ_s, and λ is the heat transfer coefficient of hot fluid, the heat transfer coefficient of cold fluid, the width of wall, thermal conductivity, respectively.

$$\Delta m_1 = k \cdot (T_h(x,t) - T_c(x,t)) \cdot (\Delta A_1) \tag{11}$$

Δm_1 is the heat flux transferring from $T_h(x,t)$ to $T_c(x,t)$. Where ΔA_1 is the heat transfer suface area $T_h(x,t)$ to $T_c(x,t)$.

$$\Delta m_2 = k \cdot (T_h(x + C, t) - T_c(x,t)) \cdot (\Delta A_2) \tag{12}$$

Δm_2 is the heat flux transferring from $T_h(x + C, t)$ to $T_c(x,t)$. Where ΔA_2 is the heat transfer surface area $T_h(x + C, t)$ to $T_c(x,t)$. Each element is of the length Δx and the heat transfer surface area $\Delta A_1, \Delta A_2$, and $\Delta A_1 \approx \Delta A_2 = \Delta A = (\Delta x) \cdot Z$, Z is the height of the spiral-plate heat exchanger, Δx is the displacement of cold fluid that moves in time Δt, $\Delta V = (\Delta x) \cdot Z \cdot \delta_h$, $\Delta t = \dfrac{\Delta x}{v_c}$. So,

$$c_c \rho_c \delta_c v_c \frac{\Delta T_c(x,t)}{\Delta x} = k(T_h(x,t) + T_h(x + C, t) - 2T_c(x,t)) \tag{13}$$

Using the thought of differential theory, the relationship between the length in the differential arc and the angle in differential arc is derived.

$$\Delta x = \sqrt{\Delta r^2 + (r(\Delta \theta))^2} \tag{14}$$

Applying the spiral function of the spiral-plate heat exchanger, $r = a\theta + b$, it is obtained from (14):

$$\Delta x = \sqrt{a^2 + (b + a\theta)^2}(\Delta \theta) \tag{15}$$

Substituting (15) into (13), the differential equation in cold fluid is obtained as follow.

$$c_c \rho_c \delta_c v_c \frac{\Delta T_c(\theta,t)}{\Delta \theta} = k\sqrt{a^2 + (b + a\theta)^2}(T_h(\theta,t) + T_h(\theta + 2\pi, t) - 2T_c(\theta,t)), \theta \in [0, 11\pi) \tag{16}$$

Because (16) is complex. we simplify (17) as follows.

$$c_c \rho_c \delta_c v_c \frac{\Delta T_c(\theta,t)}{\Delta \theta} = Fk\sqrt{a^2 + (b + a\theta)^2}(T_h(\theta,t) - T_c(\theta,t)), \theta \in [0, 11\pi) \tag{17}$$

where F is the constant between 1 and 2 relation to the shape of the heat exchanger. According to the thought of fractional order derivative [10] (17) is extended from the

integer order derivative to the fractional order derivative, we derive fractional order derivative equation in cold fluid for the spiral-plate counter-flow heat exchanger as follows. Fractional order of (18) is impacted by complex factors, it is difficult to derive by theory method.

$$c_c\rho_c\delta_c v_c D_\theta^{q2} T_c(\theta,t) = Fk\sqrt{a2 + (b + a\theta)^2}(T_h(\theta,t) - T_c(\theta,t)), \theta \in [0, 11\pi) \qquad (18)$$

With the same principle, the fractional order derivative equation in hot fluid is derived as follows.

$$c_h\rho_h\delta_h v_h D_\theta^{q1} T_h(\theta,t) = Fk\sqrt{a2 + (b + a\theta)^2}(T_c(\theta,t) - T_h(\theta,t)), \theta \in [0, 11\pi) \qquad (19)$$

$$A = \sqrt{a2 + (b + a\theta)^2} \qquad (20)$$

Nonlinear fractional order derivative equations for the spiral-plate counter-flow heat exchanger are given as follows.

$$\begin{cases} D_\theta^{q1} T_h(\theta,t) = \dfrac{kFA}{v_h c_h \rho_h \delta_h}((T_c(\theta,t) - T_h(\theta,t)) \\ D_\theta^{q2} T_c(\theta,t) = \dfrac{kFA}{v_c c_c \rho_c \delta_c}((T_h(\theta,t) - T_c(\theta,t)) \\ \theta \in [0, 11\pi] \end{cases} \qquad (21)$$

where $v_h(t)$ and $v_c(t)$ is the input flow rate of time t in hot fluid, the input flow rate of time t in cold fluid side, respectively.

$$\begin{cases} QL_1 = \delta_h Z v_h \\ QL_2 = \delta_c Z v_c \end{cases} \qquad (22)$$

where QL_1 and QL_2 is the input volume flow rate in hot fluid side and the input volume flow rate in cold fluid side, respectively. Substituting (22) into (21), fractional order derivative model for the spiral-plate counter-flow heat exchanger is described as follows.

$$\begin{cases} D_\theta^{q1} T_h(\theta,t) = \dfrac{kFAZ}{QL_1 c_h \rho_h}((T_c(\theta,t) - T_h(\theta,t)) \\ D_\theta^{q2} T_c(\theta,t) = \dfrac{kFAZ}{QL_2 c_c \rho_c}((T_h(\theta,t) - T_c(\theta,t)) \\ \theta \in [0, 11\pi] \end{cases} \qquad (23)$$

Considering initial conditions, $T_h(11\pi, t)$ and $T_c(0, t)$ is the input temperature of time t in hot fluid, the input temperature of time t in cold fluid, respectively.

3.3. Fractional Order Derivative Model for the Spiral-Plate Parallel-Flow Heat Exchanger

With the same method, the fractional order derivative model for the spiral-plate parallel-flow heat exchanger is derived as follows.

$$\begin{cases} D_\theta^{q1} T_h(\theta,t) = \dfrac{kFAZ}{QL_1 c_h \rho_h}((T_c(\theta,t) - T_h(\theta,t)) \\ D_\theta^{q2} T_c(\theta,t) = \dfrac{kFAZ}{QL_2 c_c \rho_c}((T_h(\theta,t) - T_c(\theta,t)) \\ \theta \in [0, 11\pi] \end{cases} \qquad (24)$$

Considering initial conditions, $T_h(0, t)$ and $T_c(0, t)$ is the input temperature of time t in hot fluid, the input temperature of time t in cold fluid side, respectively.

The fractional order derivation equations for the spiral-plate parallel-flow heat exchanger are similar to that with the spiral-plate counter-flow heat exchanger, but the boundary conditions are different.

4. Parallel Fractional Order Derivative Model for the Spiral-Plate Heat Exchanger and Implementation on GPU

4.1. Parallel Fractional Order Derivative Model for the Spiral-Plate Heat Exchanger

4.1.1. Parallel Model for the Spiral-Plate Counter-Flow Heat Exchanger

Applying (1)–(6) into (23), parallel fractional order derivative model for the spiral-plate counter-flow heat exchanger is described as follows.

$$
\begin{cases}
T_{hk} = (\Delta\theta)^{q_1} D_{hfrac} + B_h T_{hk-1} \\
T_{ck} = (\Delta\theta)^{q_2} D_{cfrac} + B_c T_{ck-1}
\end{cases}
\tag{25}
$$

where $T_{hk}, T_{hk-1}, D_{hfrac} \in R^N$, and $B_h \in R^{N \times N}$ $T_{ck}, T_{ck-1}, D_{cfrac} \in R^N$, and $B_c \in R^{N \times N}$

$$
T_{hk} = \begin{pmatrix} T_h(\Delta\theta) \\ T_h(2(\Delta\theta)) \\ \vdots \\ T_h(N(\Delta\theta)) \end{pmatrix}
\tag{26}
$$

$$
B_h = \begin{pmatrix}
\frac{-\Gamma(q_1+1)}{\Gamma(2)\Gamma(q_1)} & 0 & \cdots & 0 \\
\frac{\Gamma(q_1+1)}{\Gamma(3)\Gamma(q_1-1)} & \frac{-\Gamma(q_1+1)}{\Gamma(2)\Gamma(q_1)} & \cdots & 0 \\
\vdots & \vdots & \vdots & \vdots \\
\frac{(-1)^N \Gamma(q_1+1)}{\Gamma(N+1)\Gamma(q_1-N+1)} & \frac{(-1)^{(N-1)}\Gamma(q_1+1)}{\Gamma(N)\Gamma((q_1-N+1)} & \cdots & \frac{-\Gamma(q_1+1)}{\Gamma(2)\Gamma(q_1)}
\end{pmatrix}
\tag{27}
$$

$$
T_{hk-1} = \begin{pmatrix} T_h(0) \\ T_h(\Delta\theta) \\ \vdots \\ T_h((N-1)(\Delta\theta)) \end{pmatrix}
\tag{28}
$$

$$
B_c = \begin{pmatrix}
frac{-\Gamma(q_2+1)\Gamma(2)\Gamma(q_2)} & 0 & \cdots & 0 \\
\frac{\Gamma(q_2+1)}{\Gamma(3)\Gamma(q_2-1)} & \frac{-\Gamma(q_2+1)}{\Gamma(2)\Gamma(q_2)} & \cdots & 0 \\
\vdots & \vdots & \vdots & \vdots \\
\frac{(-1)^N \Gamma(q_2+1)}{\Gamma(N+1)\Gamma(q_2-N+1)} & \frac{(-1)^{(N-1)}\Gamma(q_2+1)}{\Gamma(N)\Gamma((q_2-N+1)} & \cdots & \frac{-\Gamma(q_2+1)}{\Gamma(2)\Gamma(q_2)}
\end{pmatrix}
\tag{29}
$$

$$
T_{ck} = \begin{pmatrix} T_c(\Delta\theta) \\ T_c(2\Delta\theta) \\ \vdots \\ T_c(N(\Delta\theta)) \end{pmatrix}
\tag{30}
$$

$$
T_{ck-1} = \begin{pmatrix} T_c(0) \\ T_c(\Delta\theta) \\ \vdots \\ T_c((N-1)(\Delta\theta)) \end{pmatrix}
\tag{31}
$$

So, the parallel fractional order derivative model for the spiral-plate counter-flow heat exchanger is obtained.

$$
\begin{cases}
T_{hk} = (\Delta\theta)^{q_1} \dfrac{FkZA}{QL_1 c_h \rho_h}(HT_{cK-1} - T_{hK-1}) + B_h T_{hk-1} \\
T_{ck} = (\Delta\theta)^{q_2} \dfrac{FkZA}{QL_2 c_c \rho_c}(HT_{hK-1} - T_{cK-1}) + B_c T_{ck-1} \\
T_{cout} = CT_{ck}
\end{cases}
\tag{32}
$$

$$
\begin{cases}
D_{hfrac} = \dfrac{FkZA}{QL_1 c_h \rho_h}(HT_{cK-1} - T_{hK-1}) \\
D_{cfrac} = \dfrac{FkZA}{QL_2 c_c \rho_c}(HT_{hK-1} - T_{cK-1})
\end{cases}
\tag{33}
$$

$$
\begin{cases}
T_{hk} = (\Delta\theta)^{q_1} D_{hfrac} + B_h T_{hk-1} \\
T_{ck} = (\Delta\theta)^{q_2} D_{cfrac} + B_c T_{ck-1}
\end{cases}
\tag{34}
$$

where

$$
H = \begin{pmatrix}
0 & 0 & 0 & \dots & 0 & 1 \\
0 & 0 & 0 & \dots & 1 & 0 \\
\vdots & \vdots & \vdots & \vdots & \vdots & \vdots \\
1 & 0 & 0 & \dots & 0 & 0
\end{pmatrix}
\tag{35}
$$

$$
C = \begin{pmatrix} 0 & 0 & 0 & 0 & \dots & 1 \end{pmatrix}
\tag{36}
$$

where $C \in R^{1 \times N}$ and $H \in R^{N \times N}$. The parallel fractional order derivative model for the spiral-plate counter-flow heat exchanger is a model with the parallel input data. It has high efficiency executed on GPU. The proposed parallel model is implemented on GPU by using MATLAB and CUDA [25].

4.1.2. The Proposed Parallel Model for the Spiral-Plate Parallel-Flow Heat Exchanger

The parallel fractional derivation model for the spiral-plate parallel-flow heat exchanger is obtained by the same method with the spiral-plate counter-flow heat exchanger presented as above.

From (23) with the same method, the parallel fractional order derivative equations for the spiral-plate parallel-flow heat exchanger are described as follows.

$$
\begin{cases}
T_{hk} = (\Delta\theta)^{q_1} \dfrac{FkZA}{QL_1 c_1 \rho_h}(T_{cK-1} - T_{hK-1}) + B_h T_{hk-1} \\
T_{ck} = (\Delta\theta)^{q_2} \dfrac{FkZA}{QL_2 c_c \rho_c}(T_{hK-1} - T_{cK-1}) + B_c T_{ck-1} \\
T_{cout} = CT_{ck}
\end{cases}
\tag{37}
$$

$$
\begin{cases}
D_{hfrac} = \dfrac{FkZA}{QL_1 c_h \rho_h}(T_{cK-1} - T_{hK-1}) \\
D_{cfrac} = \dfrac{FkZA}{QL_2 c_c \rho_c}(T_{hK-1} - T_{cK-1})
\end{cases}
\tag{38}
$$

The parallel fractional order derivative model for the spiral-plate parallel-flow heat exchanger is described as follow.

$$\begin{cases} T_{hk} = (\Delta\theta)^{q_1} D_{hfrac} + B_h T_{hk-1} \\ T_{ck} = (\Delta\theta)^{q_2} D_{cfrac} + B_c T_{ck-1} \end{cases} \tag{39}$$

where $T_{hk}, T_{hk-1}, D_{hfrac} \in R^N$, and $B_h \in R^{N \times N}$ $T_{ck}, T_{ck-1}, D_{cfrac} \in R^N$, and $B_c \in R^{N \times N}$.

4.2. Implementation on GPU for the Proposed Parallel Model

In this section, implementation on GPU of the proposed parallel model for the spiral-plate heat exchanger is presented. The parallel model with the parallel data has faster efficiency executed on GPU than on CPU. The thread blocks of the proposed parallel model are given in Table 2.

Table 2. The thread blocks of the proposed parallel model implemented on GPU.

Figure No.	Description
Figure 4	The thread block of the proposed parallel model
Figure 5	That of cold fluid for the counter-flow heat exchanger
Figure 6	That of hot fluid side for the counter-flow heat exchanger
Figure 7	That of cold fluid side for the parallel-flow heat exchanger
Figure 8	That of hot fluid side for the parallel-flow heat exchanger

The thread blocks of the proposed parallel model (2) implemented on GPU are shown in Figure 4.
where

$$F_k = \begin{pmatrix} f_1 \\ f_2 \\ \vdots \\ f_N \end{pmatrix} = \begin{pmatrix} f(\Delta h) \\ f(2(\Delta h)) \\ \vdots \\ f(N(\Delta h)) \end{pmatrix} \tag{40}$$

$$B = \begin{pmatrix} b_0 \\ b_1 \\ b_2 \\ \vdots \\ b_{N-1} \end{pmatrix} = \begin{pmatrix} \frac{-\Gamma(q+1)}{\Gamma(2)\Gamma(q)} & 0 & \cdots & 0 \\ \frac{\Gamma(q+1)}{\Gamma(3)\Gamma(q-1)} & \frac{-\Gamma(q+1)}{\Gamma(2)\Gamma(q)} & \cdots & 0 \\ \vdots & \vdots & \vdots & \vdots \\ \frac{(-1)^N \Gamma(q+1)}{\Gamma(N+1)\Gamma(q-N+1)} & \frac{(-1)^{(N-1)}\Gamma(q+1)}{\Gamma(N)\Gamma((q-N+1))} & \cdots & \frac{-\Gamma(q+1)}{\Gamma(2)\Gamma(q)} \end{pmatrix} \tag{41}$$
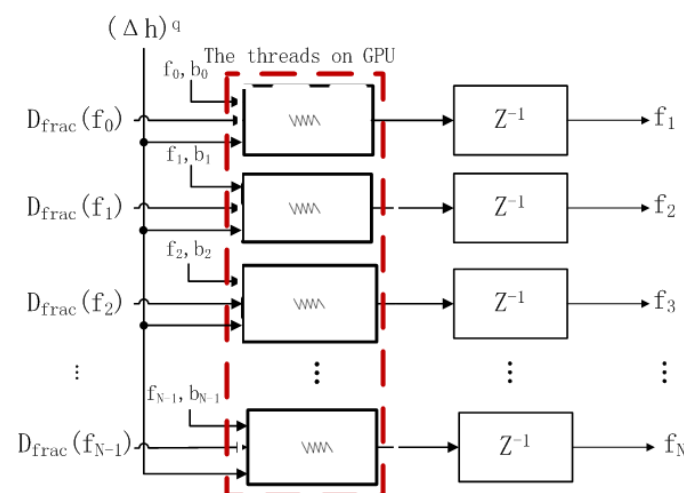

Figure 4. The thread blocks of the proposed parallel model.

$$D_{frac} = \begin{pmatrix} Df_0 \\ Df_1 \\ \vdots \\ Df_{N-1} \end{pmatrix} = \begin{pmatrix} D_t^q f(\Delta h) \\ D_t^q f(2(\Delta h)) \\ \vdots \\ D_t^q f(N(\Delta h)) \end{pmatrix} \tag{42}$$

$$F_{k-1} = \begin{pmatrix} f_0 \\ f_1 \\ f_2 \\ \vdots \\ f_{N-1} \end{pmatrix} = \begin{pmatrix} f(0) \\ f(\Delta h) \\ \vdots \\ f((N-1)(\Delta h)) \end{pmatrix} \tag{43}$$

where F_{k-1} is a parallel input data, D_{frac} is a parallel input derivation data, B is a matrix relation to the order of fractional order derivation, F_k is a parallel output data.

The thread blocks of the proposed parallel model for the spiral-plate counter-flow exchanger (32)–(34) are as shown in Figures 5 and 6.
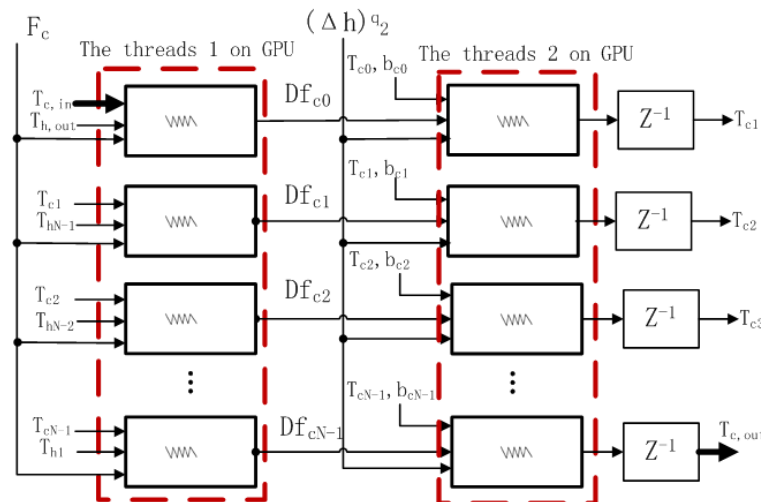
Figure 5. The thread blocks of the proposed parallel model in cold fluid for the counter-flow heat exchanger .
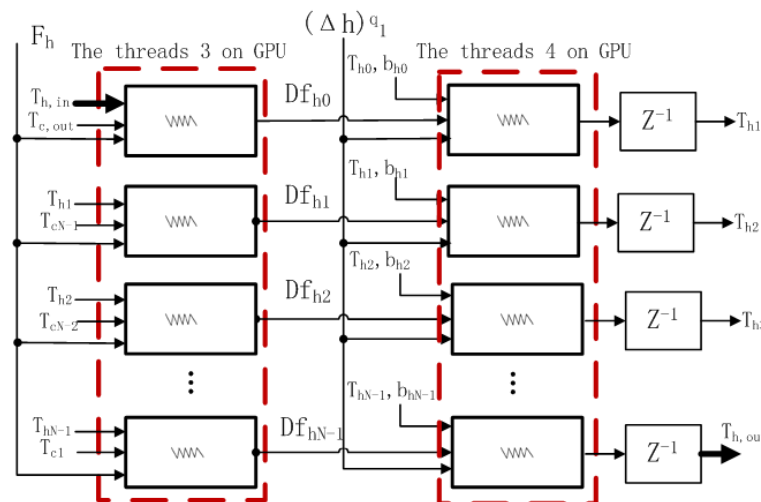
Figure 6. The thread blocks of the proposed parallel model in hot fluid for the counter-flow heat exchanger.

Here:

$$T_{ck-1} = \begin{pmatrix} T_c(0) \\ T_c(\Delta\theta) \\ \vdots \\ T_c((N-1)\Delta\theta) \end{pmatrix} = \begin{pmatrix} T_{c,in} \\ T_{c1} \\ \vdots \\ T_{cN-1} \end{pmatrix} \tag{44}$$

$$\tilde{T}_{hk-1} = HT_{hk-1} = \begin{pmatrix} T_{hN} \\ T_{hN-1} \\ \vdots \\ T_{h1} \end{pmatrix} = \begin{pmatrix} T_{h,out} \\ T_{hN-1} \\ \vdots \\ T_{h1} \end{pmatrix} \tag{45}$$

$$T_{ck} = \begin{pmatrix} T_c(\Delta\theta) \\ T_c(2(\Delta\theta)) \\ \vdots \\ T_c(N(\Delta\theta)) \end{pmatrix} = \begin{pmatrix} T_{c1} \\ T_{c2} \\ \vdots \\ T_{h,out} \end{pmatrix} \tag{46}$$

In Figure 5, $\tilde{T}_{hk-1}$ and T_{ck-1} is parallel input data, respectively. T_{ck} is a parallel output data.

$$T_{hk-1} = \begin{pmatrix} T_h(0) \\ T_h(\Delta\theta) \\ \vdots \\ T_h((N-1)\Delta\theta) \end{pmatrix} = \begin{pmatrix} T_{h,in} \\ T_{h1} \\ \vdots \\ T_{hN-1} \end{pmatrix} \tag{47}$$

$$\tilde{T}_{ck-1} = HT_{ck-1} = \begin{pmatrix} T_{cN} \\ T_{cN-1} \\ \vdots \\ T_{c1} \end{pmatrix} = \begin{pmatrix} T_{c,out} \\ T_{cN-1} \\ \vdots \\ T_{c1} \end{pmatrix} \tag{48}$$

$$T_{hk} = \begin{pmatrix} T_h(\Delta\theta) \\ T_h(2(\Delta\theta)) \\ \vdots \\ T_h(N(\Delta\theta)) \end{pmatrix} = \begin{pmatrix} T_{h1} \\ T_{h2} \\ \vdots \\ T_{c,out} \end{pmatrix} \tag{49}$$

In Figure 6, $\tilde{T}_{ck-1}$ and T_{hk-1} is parallel input data, T_{hk} is a parallel output data.

The thread blocks of proposed parallel model for the spiral-plate counter-flow exchanger (37)–(39) are as shown in Figures 7 and 8.
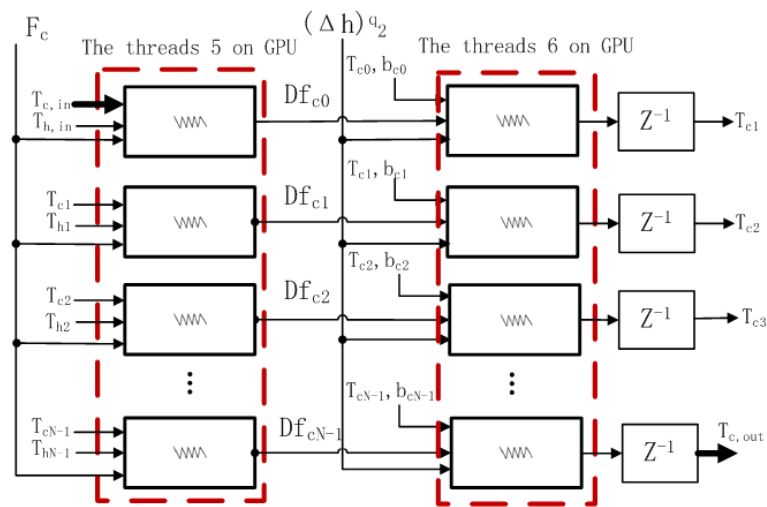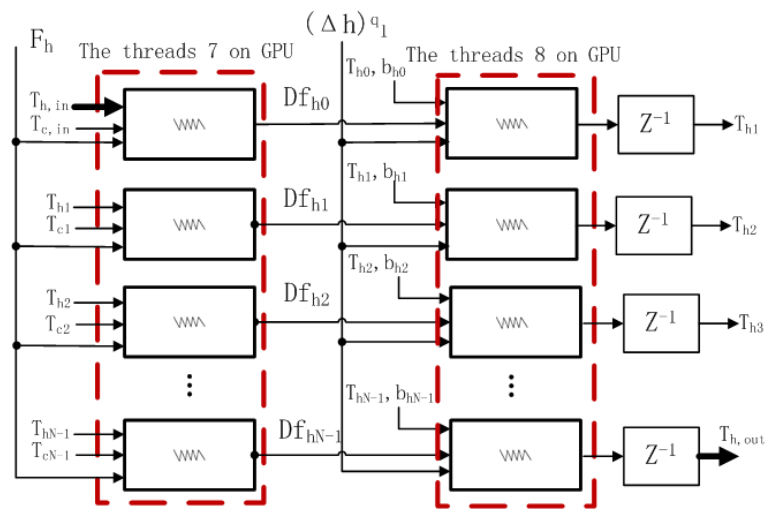
Figure 7. The thread blocks of the proposed parallel model in cold fluid for the parallel-flow heat exchanger.

Here:

$$
T_{hk-1} = \begin{pmatrix} T_h(0) \\ T_h(\Delta\theta) \\ \vdots \\ T_h((N-1)(\Delta\theta)) \end{pmatrix} = \begin{pmatrix} T_{h,in} \\ T_{h1} \\ \vdots \\ T_{hN-1} \end{pmatrix} \tag{50}
$$

$$
T_{ck-1} = \begin{pmatrix} T_c(0) \\ T_c(\Delta\theta) \\ \vdots \\ T_c((N-1)\Delta\theta) \end{pmatrix} = \begin{pmatrix} T_{c,in} \\ T_{c1} \\ \vdots \\ T_{cN-1} \end{pmatrix} \tag{51}
$$

$$
T_{ck} = \begin{pmatrix} T_c(\Delta\theta) \\ T_c(2(\Delta\theta)) \\ \vdots \\ T_c(N(\Delta\theta)) \end{pmatrix} = \begin{pmatrix} T_{c1} \\ T_{c2} \\ \vdots \\ T_{h,out} \end{pmatrix} \tag{52}
$$

$$
T_{hk} = \begin{pmatrix} T_h(\Delta\theta) \\ T_h(2(\Delta\theta)) \\ \vdots \\ T_h(N(\Delta\theta)) \end{pmatrix} = \begin{pmatrix} T_{h1} \\ T_{h2} \\ \vdots \\ T_{c,out} \end{pmatrix} \tag{53}
$$

Figure 8. The thread blocks of the proposed parallel model in hot fluid for the parallel-flow heat exchanger.

In Figure 7, T_{hk-1} and T_{ck-1} is a parallel input data, respectively. T_{ck} is a parallel output data. In Figure 8, T_{ck-1} and T_{hk-1} is a parallel input data, respectively. T_{hk} is a parallel output data. $F_h = \dfrac{FZkA}{QL_1 c_h \rho_h}$, $F_c = \dfrac{FZkA}{QL_2 c_c \rho_c}$, $T_{c,in}$, $T_{c,out}$, $T_{h,in}$, and $T_{h,out}$ is the input temperature and output temperature in cold fluid, the input temperature and the output temperature in hot fluid, respectively. Z^{-1} is a sampling delay time.

$$
B_h = \begin{pmatrix} b_{h0} \\ b_{h1} \\ \vdots \\ b_{hN-1} \end{pmatrix} \tag{54}
$$

$$
B_c = \begin{pmatrix} b_{c0} \\ b_{c1} \\ \vdots \\ b_{cN-1} \end{pmatrix} \tag{55}
$$

Therefore, parallel fractional order derivative model for the spiral-plate heat exchanger is a parallel model with the parallel input and output data. It has high execution efficiency implemented on GPU as shown Figures 4–8.

4.3. The Comparison of Execution Time for the Proposed Parallel Model on CPU and GPU

The proposed parallel model is implemented on CPU and GPU. Here, GPU (Gefore GTX 1080TI) is used to execute the proposed parallel model. In Figure 9, the comparison of execution time for the proposed parallel model on CPU and GPU is given. where $\Delta\theta$ is discretisation angle for the proposed parallel model. N is Discrete total. It shows that as the N increases, the execution time on the CPU increases, but the execution time on the GPU changes little.
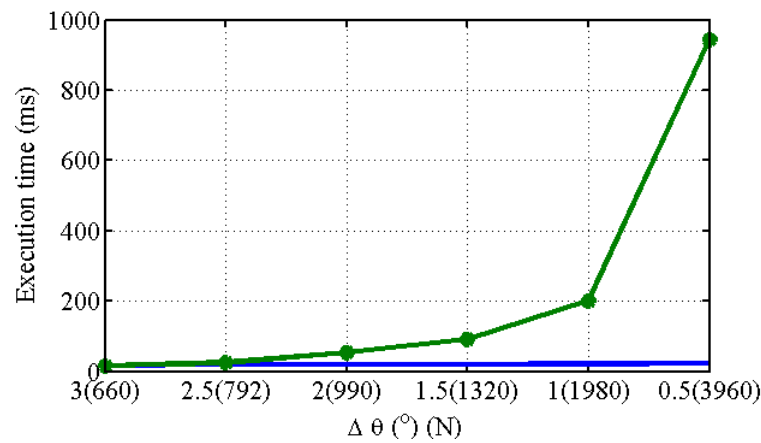
Figure 9. The comparison of execution time for the proposed parallel model on CPU and GPU.

5. Simulation on the Proposed Parallel Model for the Spiral-Plate Heat Exchanger

In this section, it is analysed for the relationships between the output temperature in cold fluid and the fractional orders q_1, q_2 for the proposed parallel model for the spiral-plate heat exchanger, the volume flow rate in hot fluid and the volume flow rate in cold fluid.

5.1. Simulation Conditions

Simulation parameters of the spiral-plate heat exchanger are shown in Table 3.

Table 3. Simulation parameters of the spiral-plate heat exchanger.

Meaning	Symbol	Value
The densities of the two fluids	ρ_c, ρ_h	1000 Kg/m^3
The specific heat capacity of the two fluids	c_c, c_h	4.2 KJ/(Kg · °C)
The input temperature of cold fluid	$T_{c,in}$	20 °C
The input temperature of hot fluid	$T_{h,in}$	50 °C
Thermal conductivity of SUS304	λ	16.7 W/(m °C)
Heat transfer coefficients of the two fluids	h_h, h_c	366 w/m^2 · K
The orders for fractional order derivative	q_1, q_2	0.9–1.02
The volume flow rate of hot fluid	QL_1	1–7 L/min
The volume flow rate of cold fluid	QL_2	1–7 L/min
Correction factor	F	1.8
Simulation time	t	[0, 12] s

5.2. Simulation on the Proposed Parallel Model for the Spiral-Plate Counter-Flow Heat Exchanger

The index of all figures for the relationships between the output temperature of cold fluid and the flow rates of hot fluid, cold fluid for the proposed parallel model of the spiral-plate counter-flow heat exchanger is shown in Table 4.

Table 4. The relationships between the output temperature of cold fluid and the volume flow rates of hot fluid, cold fluid for the proposed parallel model for the spiral-plate counter-flow heat exchanger.

Figure No.	Descrption
Figure 10	q_1, q_2 = 0.9, 0.92, 0.94, 0.96, 0.98, 1.0
Figure 11	q_1, q_2 = 1.004, 1.008, 1.01, 1.02
Figure 12	QL_1 = 1 L/min, QL_2 = 1, 3, 5, 7 L/min
Figure 13	QL_1 = 3 L/min, QL_2 = 1, 3, 5, 7 L/min
Figure 14	QL_1 = 5 L/min, QL_2 = 1, 3, 5, 7 L/min
Figure 15	QL_1 = 7 L/min, QL_2 = 1, 3, 5, 7 L/min
Figure 16	QL_1 = 1, 3, 5, 7 L/min, QL_2 = 1 L/min
Figure 17	QL_1 = 1, 3, 5, 7 L/min, QL_2 = 3 L/min
Figure 18	QL_1 = 1, 3, 5, 7 L/min, QL_2 = 5 L/min
Figure 19	QL_1 = 1, 3, 5, 7 L/min, QL_2 = 7 L/min

5.2.1. Simulation with the Different Fractional Orders as $q_1, q_2 \leq 1$

The relationships between the output temperature in cold fluid and the fractional orders as $q_1, q_2 \leq 1$ are shown in Figure 10. Those show that the output temperature increases with the fractional orders q_1, q_2 rises up as shown in Figure 10.
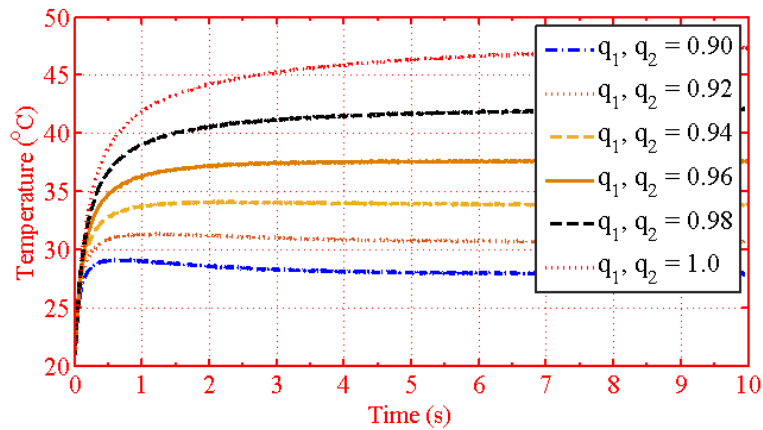

Figure 10. The output temperature in cold fluid as $q_1, q_2 \leq 1$.

5.2.2. Simulation with the Different Fractional Orders as $q_1, q_2 > 1$

The relationships between the output temperature in cold fluid and the different fractional orders as $q_1, q_2 > 1$ are shown in Figure 11. It shows when $q_1, q_2 = 1.025$, the output temperature in cold fluid is unstable.
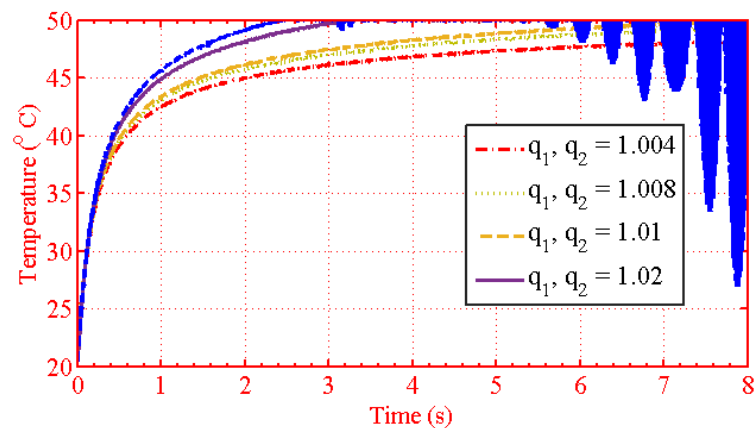
Figure 11. The output temperature in cold fluid as $q_1, q_2 > 1$.

5.2.3. The Relationships between the Output Temperature in Cold Fluid and the Different Volume Flow Rate of Hot Fluid

The relationships between the output temperature in cold fluid and the different volume flow rate of hot fluid are shown in Figures 12–15. Those figures show that the output temperature rises with the volume flow rate of hot fluid increases.
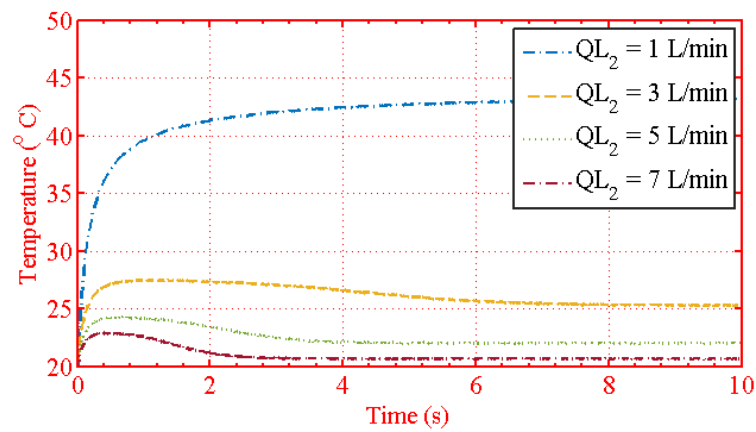
Figure 12. The output temperature in cold fluid with $QL_1 = 1$ L/min.
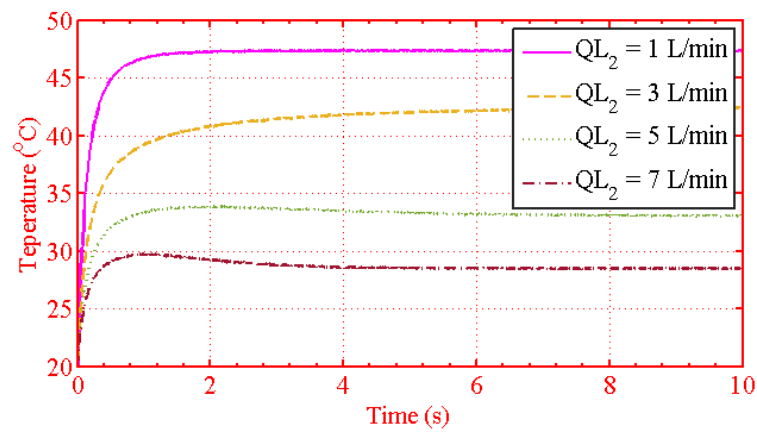
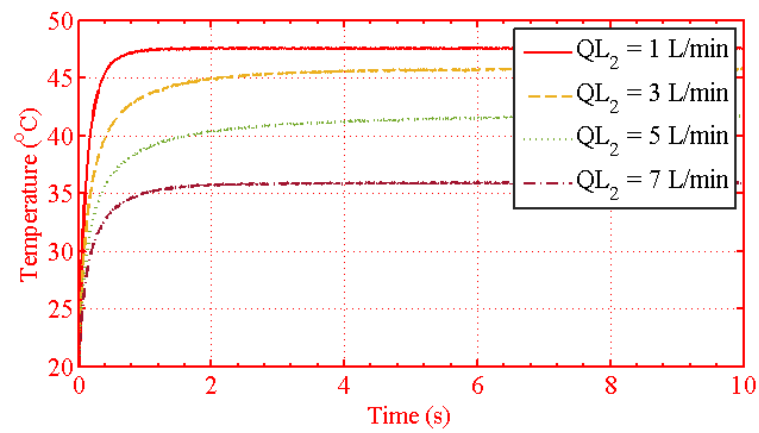**Figure 13.** The output temperature in cold fluid with $QL_1 = 3$ L/min.

Figure 14. The output temperature in cold fluid with $QL_1 = 5$ L/min.
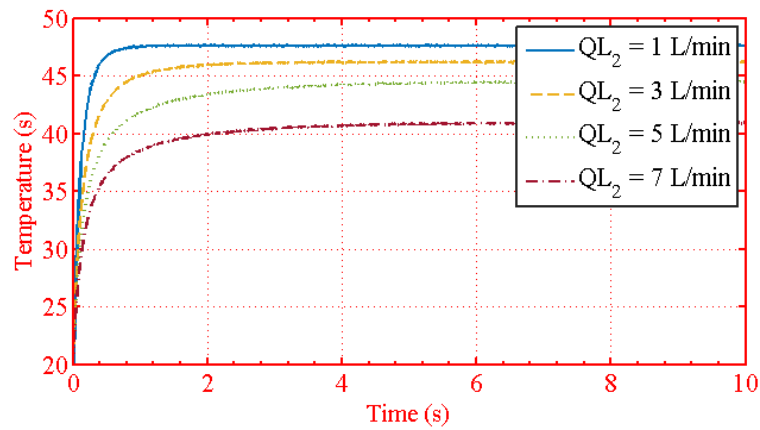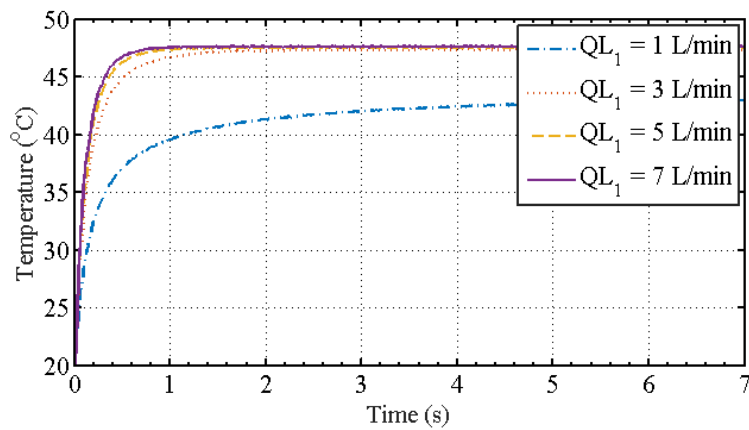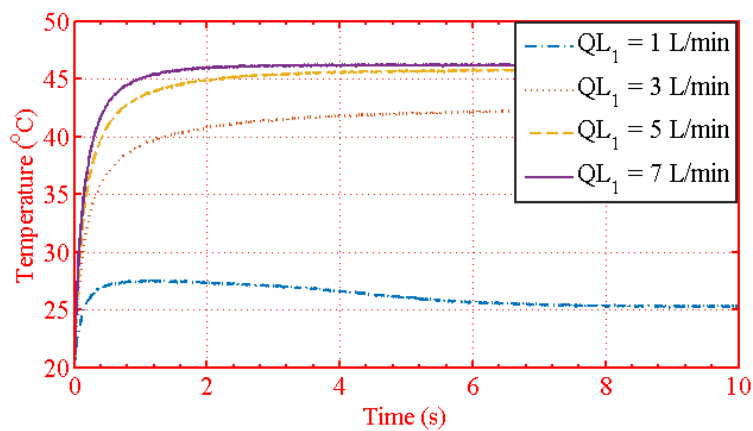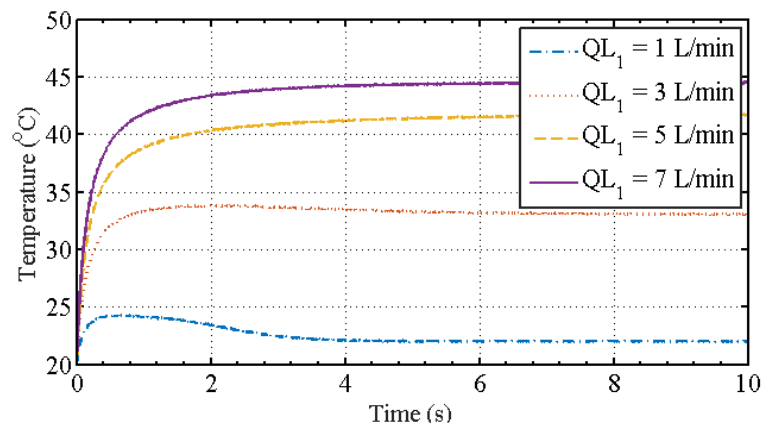
Figure 15. The output temperature in cold fluid with $QL_1 = 7$ L/min.

5.2.4. The Relationships between the Output Temperature in Cold Fluid and the Different Volume Flow Rate of Cold Fluid

The relationships between the output temperature in cold fluid and the different volume flow rate of cold fluid are shown in Figures 16–19. Those figures show that the output temperature in cold fluid goes down with the volume flow rate of cold fluid increases.

Figure 16. The output temperature in cold fluid with $QL_2 = 1$ L/min.

Figure 17. The output temperature in cold fluid with $QL_2 = 3$ L/min.

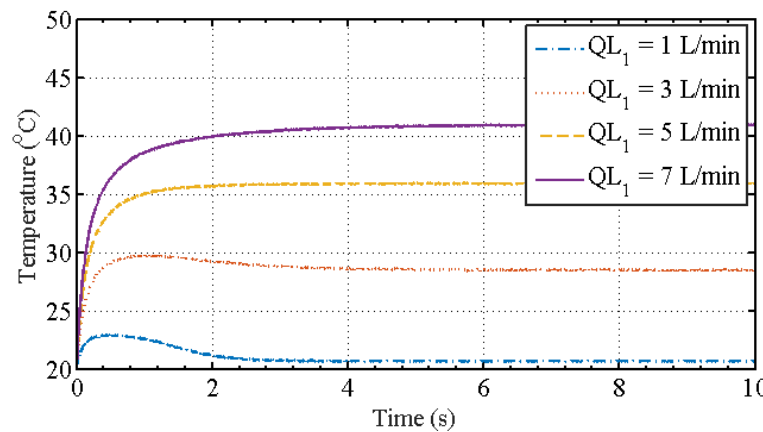**Figure 18.** The output temperature in cold fluid with QL_2 = 5 L/min.

Figure 19. The output temperature in cold fluid with QL_2 = 7 L/min.

5.3. Simulation on the Proposed Parallel Model for the Spiral-Plate Parallel-Flow Heat Exchanger

The index of all figures for the relationships between the output temperature of cold fluid and the flow rates of hot fluid, cold fluid for the proposed parallel model of the spiral-plate parallel-flow heat exchanger is shown in Table 5.

Table 5. The relationships between the output temperature of cold fluid and the flow rates of hot fluid, cold fluid for the proposed parallel model of the spiral-plate parallel-flow heat exchanger.

Figure No.	Descrption
Figure 20	q_1, q_2 = 0.9, 0.92, 0.94, 0.96, 0.98, 1.0
Figure 21	q_1 , q_2 = 1.004, 1.008, 1.01, 1.02
Figure 22	QL_1 =1 L/min, QL_2 = 1, 3, 5, 7 L/min
Figure 23	QL_1 =3 L/min, QL_2 = 1, 3, 5, 7 L/min
Figure 24	QL_1 =5 L/min, QL_2 = 1, 3, 5, 7 L/min
Figure 25	QL_1 =7 L/min, QL_2 = 1, 3, 5, 7 L/min
Figure 26	QL_1 = 1, 3, 5, 7 L/min, QL_2 = 1 L/min
Figure 27	QL_1 = 1, 3, 5, 7 L/min, QL_2 = 3 L/min
Figure 28	QL_1 = 1, 3, 5, 7 L/min, QL_2 = 5 L/min
Figure 29	QL_1 = 1, 3, 5, 7 L/min, QL_2 = 7 L/min

5.3.1. Simulation with the Different Fractional Orders as $q_1, q_2 \leq 1$

The relationships between output temperature in cold fluid and the fractional orders as $q_1, q_2 \leq 1$ are shown in Figure 20. They show that the output temperature rises with the fractional orders q_1, q_2 increases as shown in Figure 20.
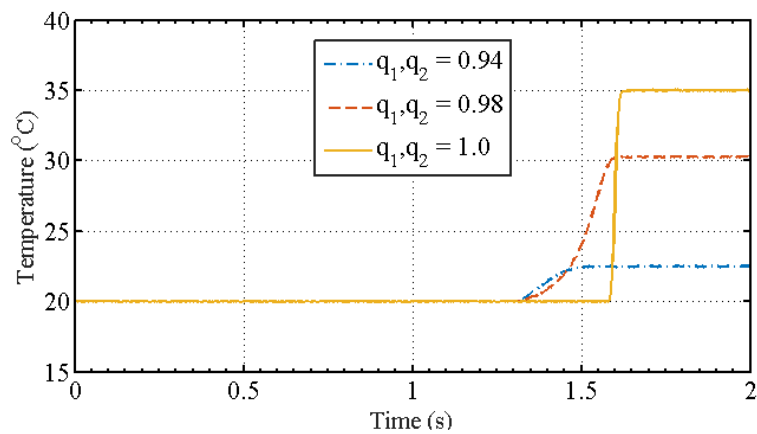
Figure 20. The output temperature in cold fluid as $q_1, q_2 \leq 1$.

5.3.2. Simulation with the Different Fractional Orders as $q_1, q_2 > 1$

The relationships between the output temperature in cold fluid and the fractional orders as $q_1, q_2 > 1$ are shown in Figure 21. When q_1, q_2 is 1.025, the output temperature in cold fluid is unstable.
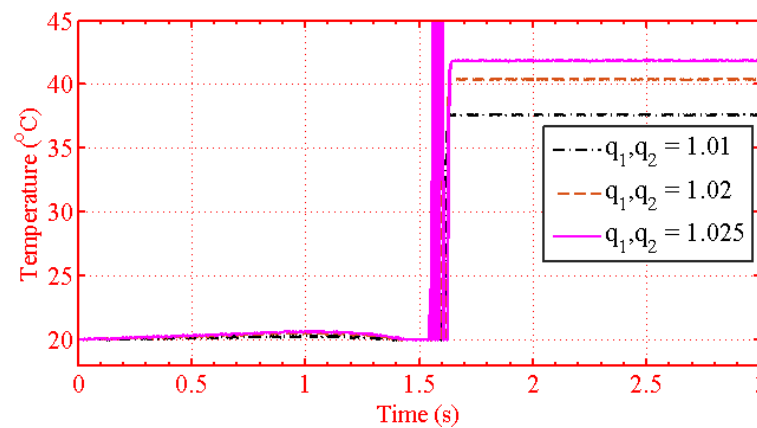

Figure 21. The output temperature in cold fluid as $q_1, q_2 > 1$.

5.3.3. The Relationships between the Output Temperature of Cold Fluid and the Different Volume Flow Rate of Hot Fluid

The relationships between the output temperature in cold fluid and the different volume flow rate of hot fluid are shown in Figures 22–25. Those figures show that output temperature in cold fluid rises with the volume flow rate of hot fluid increases.
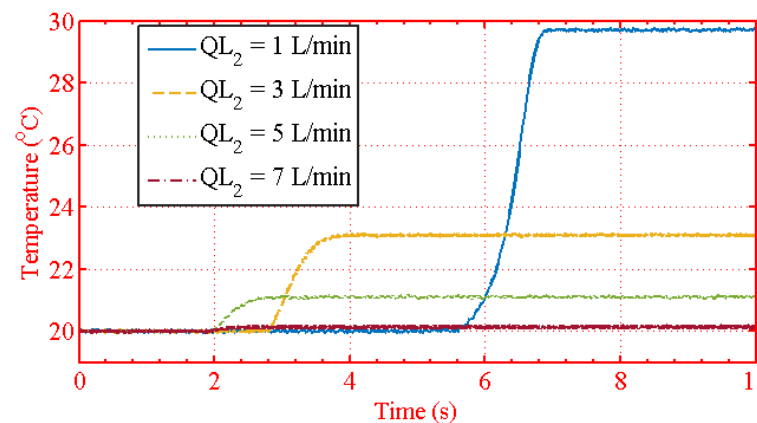

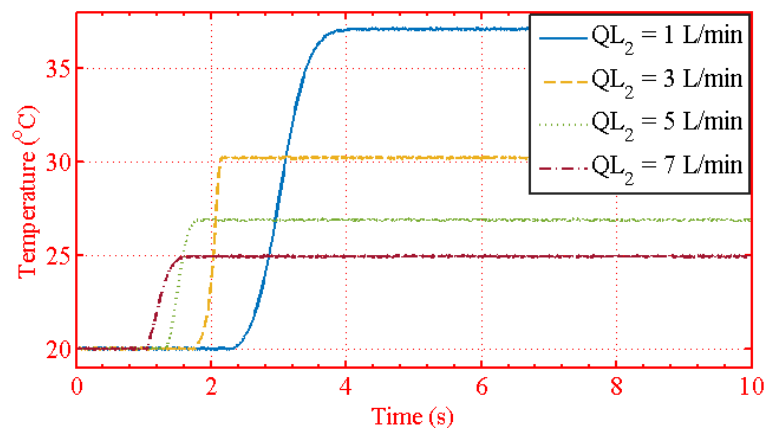**Figure 22.** The output temperature in cold fluid with $QL_1 = 1$ L/min.

Figure 23. The output temperature in cold fluid with $QL_1 = 3$ L/min.
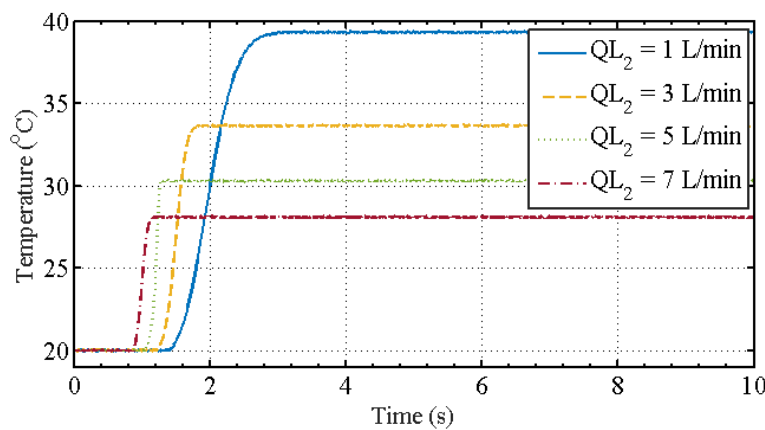

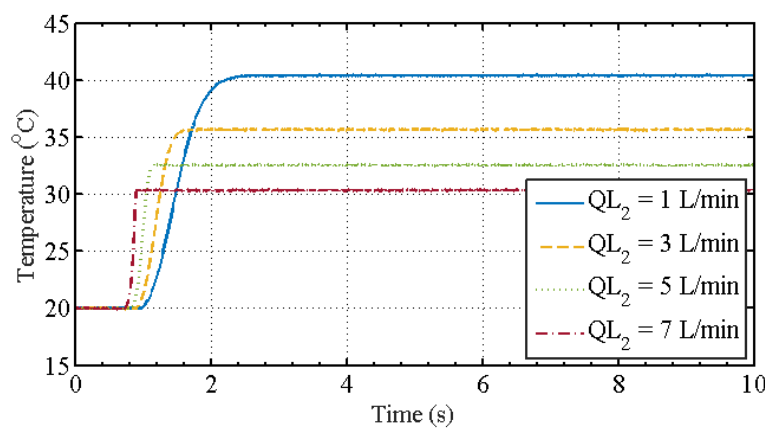**Figure 24.** The output temperature in cold fluid with $QL_1 = 5$ L/min.

Figure 25. The output temperature in cold fluid with $QL_1 = 7$ L/min.

5.3.4. The Relationships between the Output Temperature of Cold Fluid and the Different Volume Flow Rate of Cold Fluid

The relationships between the output temperature in cold fluid and the different volume flow rate of cold fluid are shown in Figures 26–29. Those figures show that the output temperature in cold fluid drops down with the volume flow rate of cold fluid increases.
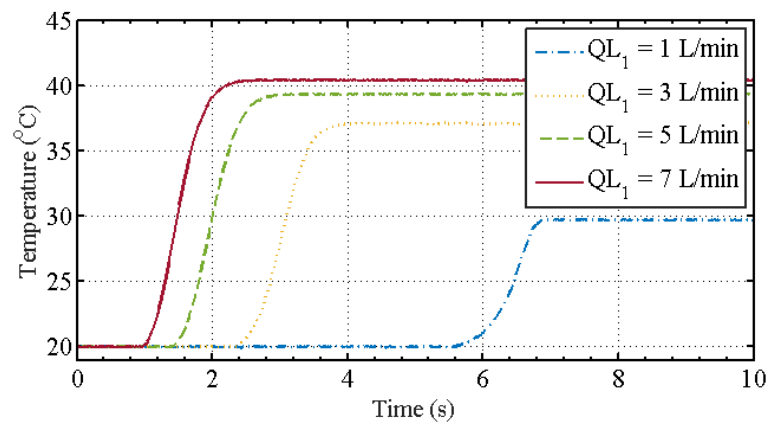
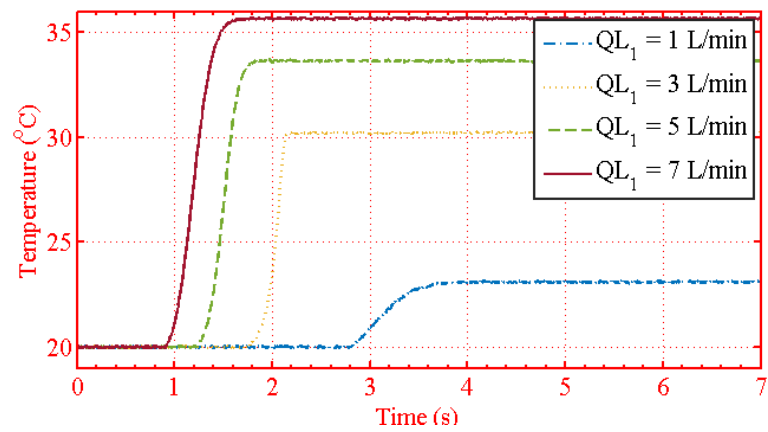**Figure 26.** The output temperature in cold fluid with $QL_2 = 1$ L/min.

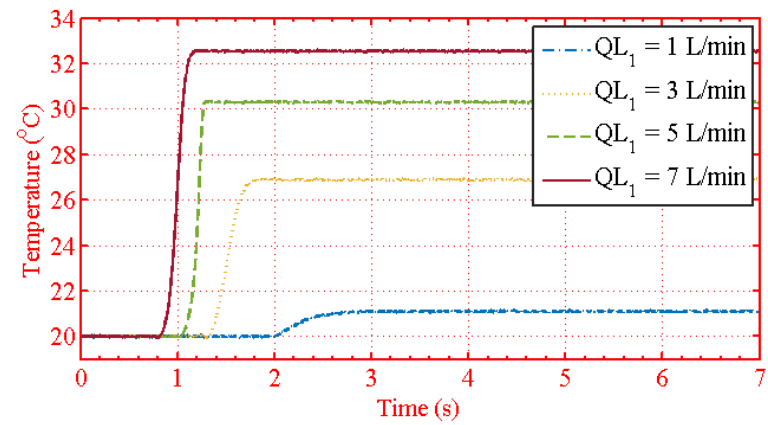**Figure 27.** The output temperature in cold fluid with $QL_2 = 3$ L/min.

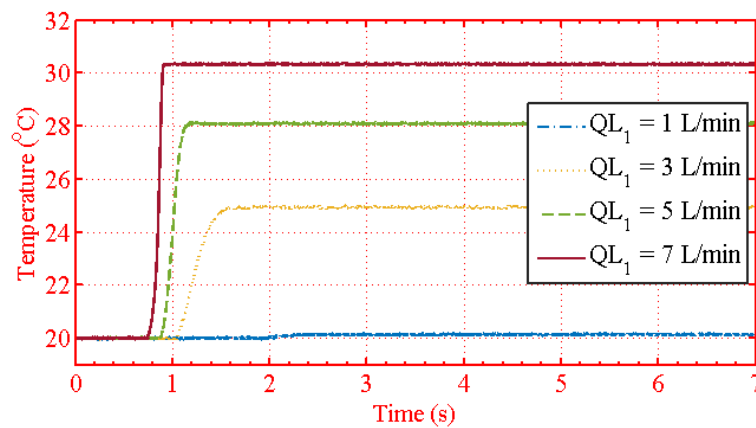**Figure 28.** The output temperature in cold fluid with $QL_2 = 5$ L/min.

Figure 29. The output temperature in cold fluid with $QL_2 = 7$ L/min.

6. Conclusions

A parallel fractional order derivative model and the problem statement are introduced in this paper. Then, the fractional order derivative model for the spiral-plate heat exchanger is constructed by mathematic analysis and extending from classical integer order derivative. Further, the parallel fractional order derivative model for the spiral-plate heat exchanger is constructed by considering the merit of GPU. Finally, the parallel fractional order derivative model for the spiral-plate heat exchanger is simulated. Simulations show the relationships between the output temperature of heated fluid and the fractional orders of the two fluids, the input volume flow rate of cold fluid, and the input volume flow rate of cold fluid, respectively.

Author Contributions: M.D. supervised the work; G.D. finished the simulation, and wrote the rest of the work. All authors have read and agreed to the published version of the manuscript.

Institutional Review Board Statement: Not applicable.

Informed Consent Statement: Not applicable.

Data Availability Statement: Not applicable.

Appendix A

Definition A1 ([10])**.** *(the Caputo's fractional order derivative)*

$$
{}^{C}_{a}D^q_t f(t) = \begin{cases} \frac{1}{\Gamma(n-q)} \int_a^t \frac{f^{(n)}(t)}{(t-\tau)^{n-q-1}} d\tau, & n-1 < q < n \\ \frac{d^n f(t)}{dt^n}, & q = n \end{cases} \tag{A1}
$$

where $\Gamma(\cdot)$ *is gamma function defined by* $\Gamma(x) = \int_0^\infty e^{-t} t^{x-1}$ *and n is a positive integer number.*

Definition A2 ([10])**.** *(the Grunwald-Letnikov's fractional order derivative)*

$$
{}^{GL}_{a}D^q_t f(t) = \lim_{\Delta h \to 0} (\Delta h)^{-q} \sum_{j=0}^{\left[\frac{t-a}{\Delta h}\right]} (-1)^j \frac{\Gamma(q+1)}{\Gamma(j+1)\Gamma(q-j+1)} f(t - j(\Delta h)) \tag{A2}
$$

where $[\cdot]$ *means the integer part.*

(A1) *and* (A2) *are equivalent if* $f(\cdot)$ *is differentiable.* (A1) *is a continues type definition of fractional order derivative.* (A2) *is a non-continues type definition of fractional order derivative.*

(A2) *is implemented easily on computer.* (A2) *is used in this paper.* (A1) *is easy to analyse system performance such as stability, tracking, etc. for the fractional order control system.*
If $\Delta h \approx 0$ then

$$
{}_{0}^{GL}D_t^q f(t) \approx (\Delta h)^{-q} \sum_{j=0}^{N} (-1)^j \frac{\Gamma(q+1)}{\Gamma(j+1)\Gamma(q-j+1)} f(t - j(\Delta h)) \tag{A3}
$$

where N is $\left[\frac{t-a}{\Delta h}\right]$.

References

1. Tapre, R.W.; Kaware, J.P. Review on heat transfer in spiral heat exchanger. *Int. J. Sci. Res.* **2015**, *5*, 1–5.
2. Sathiyan, S.; Rangarajan, M. An experimental study of spiral-plate heat exchanger for nitrobenzene-water two-phase system. *Bulg. Chem. Commun.* **2010**, *42*, 205–209.
3. Khorshidi, J.; Heidari, S. Design and construction of a spiral heat exchanger. *Adv. Chem. Eng. Sci.* **2016**, *6*, 201–298. [CrossRef]
4. Memon, S.; Gadhe, P.; Kulkarni, S. Design and testing of a spiral plate heat exchanger for textile industry. *Int. J. Sci. Eng. Res.* **2019**, *10*, 149–157.
5. Metta, V.R.; Konijeti, R.; Dasore, A. Thermal design of spiral plate heat exchanger through numerical modelling. *Int. J. Mech. Eng. Technol.* **2018**, *9*, 736–745.
6. Gomadam, P.M.; White, R.E.; Weidner, J.W. Modeling heat conduction in spiral geometries. *J. Electrochem. Soc.* **2003**, *150*, A1339–A1345. [CrossRef]
7. Bidabadi, M.; Sadaghiani, A.K.; Azad, A.V. Spiral heat exchanger optimization using genetic algorithm. *Sci. Iran. B* **2013**, *20*, 1445–1454.
8. Wen, S.; Deng, M. Operator-based robust nonlinear control and fault detection for a Peltier actuated thermal process. *Math. Comput. Model.* **2012**, *57*, 16–29. [CrossRef]
9. Fujii, R.; Deng, M.; Wakitani, S. Nonlinear remote temperature control of a spiral plate heat exchanger. In Proceedings of the 2015 International Conference on Advanced Mechatronic Systems, Beijing, China, 22–24 August 2015; pp. 533–537.
10. Podlubny, I. *Fractional Differential Equations*; Academic Press: Cambridge, MA, USA, 1999.
11. Jafari, H.; Khalique, C.M.; Nazari, M. An algorithm for the numerical solution of nonlinear fractional-order Van der Pol oscillator equation. *Math. Comput. Model.* **2012**, *55*, 1782–1786. [CrossRef]
12. Ibrahim, R.W.; Darus, M. On a new solution of factional differential equation using complex transform in the unit disk. *Math. Comput. Appl.* **2014**, *19*, 152–160.
13. Qian, D.; Li, C.; Agarwal, R.P. Stability analysis of fractional differential system with Riemann–Liouville derivative. *Math. Comput. Model.* **2010**, *52*, 862–874.
14. Baranowski, J.; Zagorowska, M.; Bauer, W.; Dziwinski, T.; Piatek, P. Applications of Direct Lyapunov Method in Caputo Non-Integer Order Systems. *Elektron. Elektrotechnika* **2015**, *21*, 10–13. [CrossRef]
15. Li, Y.; Chen, Y.; Podlubny, I. Mittag–Leffler stability of fractional order nonlinear dynamic systems. *Automatica* **2009**, *45*, 1965–1969. [CrossRef]
16. Caponetto, R.; Dongola, G.; Fortuna, L.; Petras, I. *Fractional Order Systems: Modeling and Control Applications*; World Scientific: Singapore, 2010.
17. Patnaik, S.; Sidhardh, S.; Semperlotti, F. Nonlinear thermoelastic fractional-order model of nonlocal plates: Application to postbuckling and bending response. *Thin-Walled Struct.* **2021**, *164*, 107809. [CrossRef]
18. Challamel, N.; Zorica, D.; Atanacković, T.M.; Spasić, D.T. On the fractional generalization of Eringen's nonlocal elasticity for wave propagation. *Comptes Rendus Mécanique* **2013**, *341*, 298–303. [CrossRef]
19. Sidhardh, S.; Patnaik, S.; Semperlotti, F. Thermodynamics of fractional-order nonlocal continua and its application to the thermoelastic response of beams. *Eur. J. Mech. A/Solids* **2021**, *88*, 104238. [CrossRef]
20. Monje, C.A.; Chen, Y.; Vinagre, B.M.; Xue, D.; Feliu, V. *Fractional Order Systems and Controls: Fundamentals and Applications*; Springer: Berlin/Heidelberg, Germany, 2010.
21. Oldham, K.B.; Spanier, J. *The Fractional Calculus: Theory and Applications of Differentiation and Integration to Arbitrary Order*; Dover Publications: Mineola, NY, USA, 2006.
22. Magin, R.L.; Ovadia, M. Modeling the cardiac tissue electrode interface using fractional calculus. *J. Vib. Control* **2008**, *14*, 1431–1442. [CrossRef]
23. Padovan, J. Computational algorithms for FE formulations involving fractional operator. *Comput. Mech.* **1987**, *2*, 271–287. [CrossRef]
24. Zhong, L. Comparative analysis of GPU and CPU. *Technol. Mark.* **2009**, *9*, 13–14.
25. Liu, S.; Liu, M.; Zhang, G. Model of accelerating MATLAB computation based on CUDA. *Appl. Res. Comput.* **2010**, *6*, 2140–2143.
26. Povstenko, Y. *Fractional Thermoelasticity*; Springer International Publishing: Berlin/Heidelberg, Germany, 2015.

27. Challamel, N.; Grazide, C.; Picandet, V.; Perrot, A.; Zhang, Y. A nonlocal Fourier's law and its application to the heat conduction of one-dimensional and two-dimensional thermal. *Comptes Rendus Mécanique* **2016**, *344*, 388–401. [CrossRef]
28. Sumelka, W. Thermoelasticity in the Framework of the Fractional Continuum Mechanics. *J. Therm. Stress.* **2014**, *37*, 678–706. [CrossRef]
29. Deng, M.; Wen, S.; Inoue, A. Operator-based robust nonlinear control for a Peltier actuated process. *Meas. Control. J. Inst. Meas. Control.* **2011**, *44*, 116–120. [CrossRef]
30. Bi, S.; Deng, M.; Xiao, Y. Robust Stability and Tracking for Operator-Based Nonlinear Uncertain Systems. *IEEE Trans. Autom. Sci. Eng.* **2015**, *12*, 1059–1066. [CrossRef]
31. Deng, M.; Kawashima, T. Adaptive Nonlinear Sensorless Control for an Uncertain Miniature Pneumatic Curling Rubber Actuator Using Passivity and Robust Right Coprime Factorization. *IEEE Trans. Control Syst. Technol.* **2016**, *24*, 318–324. [CrossRef]
32. Dong, G.; Deng, M. Modeling of a spiral heat exchanger using fractional order equation and GPU. In Proceedings of the 2019 International Conference on Advanced Mechatronic Systems (ICAMechS), Kusatsu, Japan, 26–28 August 2019; pp. 108–113.
33. Magadum, A.; Pawar, A.; Patil, R.; Phadtare, R.; Mestri, T.C. Review of experimental analysis of parallel and counter flow heat exchanger. *Int. J. Eng. Res. Technol.* **2016**, *5*, 395–397.
34. Bergman, T.; Lavine, A.; Incropera, F.; Dewitt, D. *Faundamentals of Heat and Mass Transfer*, 8th ed.; Wiley: Hoboken, NJ, USA, 2017.